

Cellular and Molecular Life Sciences

The linker region of breast cancer resistance protein ABCG2 is critical for coupling of ATP-dependent drug transport --Manuscript Draft--

Manuscript Number:	CMLS-D-15-00691R1	
Full Title:	The linker region of breast cancer resistance protein ABCG2 is critical for coupling of ATP-dependent drug transport	
Article Type:	Original Article	
Corresponding Author:	Attilio Di Pietro Institute of Protein Biology and Chemistry Lyon, FRANCE	
Corresponding Author Secondary Information:		
Corresponding Author's Institution:	Institute of Protein Biology and Chemistry	
Corresponding Author's Secondary Institution:		
First Author:	Attilio Di Pietro	
First Author Secondary Information:		
Order of Authors:	Attilio Di Pietro	
	Sira Macalou, PhD	
	Robert W. Robey, PhD	
	Gustavo Jabor Gozzi, Master	
	Suneet Shukla, PhD	
	Isabelle Grosjean, Master	
	Tamas Hegedus, PhD	
	Suresh V. Ambudkar, PhD	
	Susan E. Bates, MD	
Order of Authors Secondary Information:		
Funding Information:	CNRS and University of Lyon (UMR 5086)	Dr. Attilio Di Pietro
	French National Ligue against Cancer (Equipe Labellisée 2009-2014)	Dr. Attilio Di Pietro
	Région Rhône-Alpes (Explora'Doc)	Sira Macalou
	French Association of Research on Cancer (PhD fellowship)	Sira Macalou
	Intramural Research Program of the NIH, NCI, Center for Cancer Research	Susan E. Bates
Abstract:	<p>The ATP-binding cassette (ABC) transporters of class G display a different domain organisation than P-glycoprotein/ABCB1 and bacterial homologues with a nucleotide-binding domain preceding the transmembrane domain. The linker region connecting these domains is unique and its function and structure cannot be predicted. Sequence analysis revealed that the human ABCG2 linker contains a LSGGE sequence, homologous to the canonical C motif/ABC signature present in all ABC nucleotide-binding domains. Predictions of disorder and of secondary structures indicated that this C2-sequence was highly mobile and located between an α-helix and a loop similarly to the C-motif. Point mutations of the two first residues of the C2 sequence fully abolished the transport-coupled ATPase activity, and led to the complete loss of cell resistance to</p>	

	mitoxantrone. The interaction with potent, selective and non-competitive, ABCG2 inhibitors was also significantly altered upon mutation. These results suggest an important mechanistic role for the C2-sequence of the ABCG2 linker region in ATP binding and/or hydrolysis coupled to drug efflux.
Response to Reviewers:	See attachment entitled "Detailed answers to reviewer's comments"

The linker region of breast cancer resistance protein ABCG2 is critical for coupling of ATP-dependent drug transport

**S. Macalou, R. W. Robey, G. Jabor Gozzi, S. Shukla, I. Grosjean, T. Hegedus, S.
V. Ambudkar, S. E. Bates, A. Di Pietro**

S. Macalou, G. Jabor Gozzi, A. Di Pietro (✉)

Equipe Labellisée Ligue 2014, BMSSI, UMR 5086 CNRS-Université Lyon 1, IBCP,
69007 Lyon, France

e-mail: a.dipietro@ibcp.fr

R. W. Robey, S. E. Bates

Medical Oncology Branch, Center for Cancer Research, National Cancer Institute,
National Institutes of Health, Bethesda, MD 20892, USA

S. Shukla, S. V. Ambudkar

Laboratory of Cell Biology, Center for Cancer Research, National Cancer Institute,
National Institutes of Health, Bethesda, MD 20892, USA

I. Grosjean

CelluloNet biobank BB-0033-00072 facility of UMS3444/US8/SFR Biosciences,
IBCP, 69007 Lyon, France

T. Hegedus

MTA-SE Molecular Biophysics Research Group, Hungarian Academy of Sciences
and Department of Biophysics and Radiation Biology, Semmelweis University,
Budapest, Hungary.

Running title: Linker region of human ABCG2

Keywords: ABC transporter, breast cancer resistance protein/ABCG2, ATP
hydrolysis, C motif/ABC signature, drug efflux coupling, specific sequence.

Abbreviations: ABC, ATP-binding cassette; MDR, multidrug resistance

Abstract

The ATP-binding cassette (ABC) transporters of class G display a different domain organisation than P-glycoprotein/ABCB1 and bacterial homologues with a nucleotide-binding domain preceding the transmembrane domain. The linker region connecting these domains is unique and its function and structure cannot be predicted. Sequence analysis revealed that the human ABCG2 linker contains a LSGGE sequence, homologous to the canonical C-motif/ABC signature present in all ABC nucleotide-binding domains. Predictions of disorder and of secondary structures indicated that this C2-sequence was highly mobile and located between an α -helix and a loop similarly to the C-motif. Point mutations of the two first residues of the C2-sequence fully abolished the transport-coupled ATPase activity, and led to the complete loss of cell resistance to mitoxantrone. The interaction with potent, selective and non-competitive, ABCG2 inhibitors was also significantly altered upon mutation. These results suggest an important mechanistic role for the C2-sequence of the ABCG2 linker region in ATP binding and/or hydrolysis coupled to drug efflux.

Introduction

The ABCG2 transporter was discovered simultaneously in three different groups; it was called ABCP for its abundance in placenta [1], BCRP as a breast cancer resistance protein [2] and MXR for its induced resistance to mitoxantrone [3]. Its overexpression in cancer cells was identified to strongly contribute to multidrug resistance, similarly to previously discovered P-glycoprotein/ABCB1 [4, 5] and MRP1/ABCC1 [6]. ABCG2 also plays an essential physiological control within barriers protecting sensitive organs [7, 8] as well as in stem cells of which it is considered to be a marker [9].

All members of the ATP-binding cassette (ABC) superfamily are constituted of cytosolic nucleotide-binding domains (NBDs), responsible for ATP binding and hydrolysis, and two transmembrane domains (TMDs) generally comprising 6 α -helical spans ensuring substrate transport across the membrane. These four domains are fused through linkers into a single **TMD1-NBD1-TMD2-NBD2** polypeptide, as a “full-transporter” in P-glycoprotein (ABCB1) and MRP1 (**which** also contains an additional **N-terminal TMD0** domain). In contrast **to ABCB1 and MRP1**, ABCG2 is a “half-transporter”, with a single NBD fused to a single TMD, and therefore requires dimerization, at a minimum, to form a functional unit. **Its NBD-TMD** domain arrangement is **different; as** a consequence, the linker connecting both domains is unique and its structure cannot be modeled using a template, such as the crystal structures of P-glycoproteins from mice [10] or *Caenorhabditis elegans* [11], or of a bacterial homologue [12].

All NBDs of the ABC transporters contain several ATP-binding motifs: in addition to the Walker-A and Walker-B motifs also present in other ATPases, a conserved specific sequence LSGGQ, followed by three basic residues, is called “C-motif” or “C-loop” and is considered to be an “ABC signature”. Its critical function in

ATP hydrolysis and in coupled substrate transport was demonstrated by site-directed mutagenesis in various transporters such as P-glycoprotein [13, 14], MRP1 [15], TAP [16, 17] and MalK [18]. The crystal structure of HlyB precisely identified the interactions with different moieties (adenine, ribose and γ -phosphate) of bound ATP, and additionally showed protein-protein interactions with the Walker-A motif of the other NBD [19]. The C-motif is therefore contributing to NBD dimerization, which is required for ATP hydrolysis and its coupling to the transport process by two types of direct interactions: (1) with ATP, mainly bound to the other NBD through Walker-A, Walker-B and other motifs, and (2) with the Walker-A motif of the other NBD.

In the present work, an additional C-motif LSGGE, called the C2-sequence, was identified at positions 352-356, within the poorly known linker region of human ABCG2. The aim was therefore to look at its conservation among ABCGs and species, and a potential function. The results show that the C2-sequence is predicted to be quite mobile and structurally similar to the C-motif; point mutations fully altered ABCG2-mediated coupled ATPase activity and cellular multidrug resistance, suggesting a critical role in coupling between ATP hydrolysis and drug efflux.

Materials and Methods

Sequence alignment and structure predictions

Sequences were downloaded from UniProt [20]. Sequence alignments were generated using ClustalW using default parameters [21], analyzed and displayed in Cinema5 (<http://aig.cs.man.ac.uk/research/utopia/cinema/cinema.php>). Sequences were queried for the ABC signature pattern (ProSite; <http://prosite.expasy.org/PDOC00185>) employing the preg software from EMBOSS (The European Molecular Biology Open Software Suite) [22]. Two conceptually different algorithms were used to predict disorder tendency with default parameters

including DISOPRED2 [23] and IUPRED [24]. Secondary structure prediction was done employing also different predictors: Prof (<http://www.aber.ac.uk/~phiwww/prof/>), Jnet [25] and PSI [26].

Compounds

Commercial reagents were of the highest available purity grade: mitoxantrone ($\geq 97\%$) and Ko143 ($\geq 98\%$) were purchased from Sigma-Aldrich (France), and nilotinib from Selleck Chemicals (Boston, MA). Chromone 1 was obtained as previously described [27]. The 5D3 monoclonal antibody was purchased from eBioscience and BXP-21 antibody from Alexis Biochemicals.

Generation of Mutants

The L352A, S353A, G354A, G355A and E356A point mutants were generated by site-directed mutagenesis in a pcDNA3.1 vector (Invitrogen) carrying the full length *ABCG2* cDNA, kindly provided by the laboratory of Dr. Douglas Ross. Site-directed mutagenesis was carried out using the "QuickChange® Site-Directed Mutagenesis" kit (Stratagene). The plasmid containing *ABCG2* was amplified by PCR from primers containing the desired mutation. The full-length sequences of all mutant constructs were tested for correctness by sequencing. The designed primer sequences are presented in the following table, where the mutated nucleotides are in bold letters.

Primers	Sequences
L352A-Fw	ACAAAAGCTGAATTACATCAAG G CTTCCGGGGGTGAGAAG
L352A-Rv	CTTCTCACCCCCGGAAG G CTTGATGTAATTCAGCTTTTGT
S353A-Fw	AAAGCTGAATTACATCAACTT G CCGGGGGTGAGAAGAAG
S353A-Rv	CTTCTTCTCACCCCCGG C AAGTTGATGTAATTCAGCTTT
G354A-Fw	CCTGAATTACATCAACTTTCCG C GGGTGAGAAGAAGAAG
G354A-Rv	CTTCTTCTTCTCACCC G CGGAAAGTTGATGTAATTCAGG

G355A-Fw TTACATCAACTTTCCGGGGCTGAGAAGAAGAAGAAGATC

G355A-Rv GATCTTCTTCTTCTTCTCAGCCCCGGAAAGTTGATGTAA

E356A-Fw TTACATCAACTTTCCGGGGGTGCGAAGAAGAAGAAGATC

E356A-Rv GATCTTCTTCTTCTTCTCGCACCCCCGGAAAGTTGATGTAA

Cell cultures

Human Embryonic 293 cell line (CelluloNet n°109) was transfected (Nucleofector technique, solution 5, programme A23, LONZA) with either ABCG2 (HEK293-ABCG2, also called “293BCRP3, CelluloNet n° 234”) or the empty vector (HEK293-*pcDNA3*) or ABCG2 mutants. Stable polyclonal cell lines were then selected with 0.75mg/ml G418, and cell lines were cloned. They were maintained in high-glucose DMEM supplemented with 10% fetal bovine serum (FBS), 1% penicillin/streptomycin at 37 °C, 5% CO₂ under controlled humidity. The cell culture medium was supplemented with 0.75 mg/mL G418.

5D3 binding

In studies with the anti-ABCG2 antibody 5D3, cells were incubated in 2% BSA/DPBS (Dulbecco’s Phosphate Buffered Saline) with either phycoerythrin-labeled negative control antibody (IgG2b) or phycoerythrin-labeled 5D3 antibody (both from eBioscience, San Diego, CA), used in excess according to the manufacturer’s instructions, washed with DPBS, and subsequently analyzed. Surface expression of ABCG2 was calculated as the difference in mean channel numbers between the 5D3 histogram and the negative-control antibody histogram. Samples were analyzed on a FACSsort flow cytometer (Becton Dickinson, San Jose, CA). Phycoerythrin fluorescence was detected with a 488 nm argon laser and a 585 nm bandpass filter. At least 10,000 events were collected for each flow cytometry experiment. By gating

on forward *versus* side scatter, debris was eliminated, and dead cells were excluded based on propidium iodide staining.

Mitoxantrone efflux and inhibition by characteristic inhibitors

HEK-293 cells expressing wild-type or mutated ABCG2 were trypsinized and incubated for 30 min with 20 μ M mitoxantrone in the presence or absence of 10 μ M of the ABCG2 inhibitor fumitremorgin C (FTC). Cells were then washed and incubated for 1 h in mitoxantrone-free medium continuing with or without FTC. Mitoxantrone efflux was calculated by subtracting the mean fluorescence of the cells incubated without FTC from the mean fluorescence of the cells incubated with FTC as previously described [28].

Cell growth resistance to mitoxantrone

HEK-293 cells expressing wild-type or mutated ABCG2, as well as control cells were seeded at a density of 10^4 cells/well into 96-well culture plates, incubated overnight, and treated with mitoxantrone (up to 1 μ M) for 72 h. To assess viability, the cells were exposed to 0.5 mg/mL MTT and incubated for 4 h at 37 °C [29]. The culture medium was discarded, and 100 μ L of a DMSO/ethanol (1:1) solution was added into each well and mixed by gently shaking for 10 min. Absorbance was measured at 570 nm using a microplate reader, and the value measured at 690 nm was subtracted. Data are the mean \pm SD of at least three independent experiments.

ATPase activity assay

Beryllium-fluoride-sensitive ATPase activity was assayed using crude membranes (10 μ g protein/tube) of HEK293 cells expressing WT and mutant ABCG2 as described previously [30]. Briefly crude membranes isolated from HEK cells

expressing ABCG2 (1 mg of protein/ml) were incubated at 37°C in ATPase assay buffer (50 mM KCl, 5 mM sodium azide, 2 mM EGTA, 1 mM ouabain, 10 mM MgCl₂, 2 mM dithiothreitol, and 50 mM Tris-MES, pH 6.8) in the presence or absence of indicated substrates for 5 min. The ATPase reaction was started by the addition of 5 mM ATP and was terminated by the addition of 0.1 ml SDS solution after 20 min. The amount of inorganic phosphate released was quantified by a colorimetric reaction as described previously [30].

Results

Identification of a specific C2-sequence in human ABCG2

Sequence alignment of the different human ABCG transporters indicated the following consensus for the canonical ABC signature/C-motif, L/V-S-G-G-E/Q followed by R-K/R-R (Fig. 1A), **except for some degenerescence in ABCG5 which is functionally active as an heterodimer with ABCG8**. The ABCG2 sequence located at positions 188-192 **was V-S-G-G-E**. Quite interestingly, a very similar additional sequence, called hereafter C2-sequence (L-S-G-G-E, followed by K-K-K), was found exclusively in human ABCG2, at positions 352-356 (Fig. 1B). It obeyed the consensus sequence illustrated here above for human ABCG members, and known to be common to all ABC transporters; it could therefore be defined as an extra, non-canonical, C-motif. Sequence alignment of human ABCG2 with ABCG2 homologues from different species indicated in Fig. 1C that this non-canonical human C2-sequence was well conserved in mammals (elephant, dog, horses, goat, bovines, ovines, primates and rodents), partly in avian organisms (chicken, turkey) and in amphibia, but not in fishes, protozoan parasites and plants. Interestingly, no C2-sequence was found in yeast MDR full-transporters, with similar **domain organisation**

as ABCG2, such as *Saccharomyces cerevisiae* Pdr5p or *Candida albicans* Cdr1p (not shown).

Secondary structure predictions indicate the C2-sequence located at the border of an α -helix and a region without stable secondary structure similarly as the canonical C-motif. Moreover, the latter segment around a.a. 360 is predicted to be the most disordered part of the 301-396 linker region when using the DISPORED2 program, and one among the regions with higher disorder tendency determined by the IUPred program (Fig. 2). The coherence of the secondary structure and disorder predictions employing different algorithms strengthens the hypothesis that the C2-sequence can be embedded into a similar structural environment as the canonical C-motif.

Slight alterations of C2-sequence mutations on cell surface expression and activity of ABCG2

Single point mutation into alanine of each of the five residues of the C2-sequence (L352-S353-G354-G355-E356) induced variable consequences on the total ABCG2 expression monitored by Western blotting with the BXP-21 ABCG2-specific antibody: from at least 2-fold decrease *versus* the wild-type protein for L352A, S353A and E356A mutants, to no apparent effect for the G354A and G355A mutants (not shown here). However, the plasma membrane expression of ABCG2, as monitored with the 5D3 antibody recognizing the ABCG2 extracellular loop 3, was hardly modified except for the S353A mutant exhibiting a decrease of 13% (Fig. 3A-B). The correct trafficking to plasma membrane was visualized and confirmed by confocal microscopy (Fig. 3C). Mitoxantrone efflux was measured by flow cytometry as differential intracellular accumulation (Fig. 4A-B) and was also corrected for the small differences observed in membrane expression: the two L352A and S353A mutants

showed a moderate decrease of 23-32% in activity when compared to that of the wild-type ABCG2 (Fig. 4C). Symmetrically, a positive control with the gain-of-function R482G mutant showed a marked increase in mitoxantrone efflux: about 45% *versus* wild-type ABCG2, and 90-115% *versus* the two L352A and S353A mutants.

C2-mutants exhibit a markedly decreased resistance to mitoxantrone

The consequences of point mutations were much more pronounced in 72 h long cytotoxicity assays, performed in the presence of mitoxantrone and quantified by a cell survival MTT test. A complete loss of resistance to mitoxantrone cytotoxicity was observed with both L352A (Fig. 5A) and S353A (Fig. 5B) mutants, both of which reached sensitivity levels similar to that of the ABCG2-negative HEK-293 control cells transfected with the empty pcDNA3.1 vector. A lower, but significant, chemosensitization was observed with the G354A (Fig. 5C) and E356A (Fig. 5D) mutants.

Alterations of basal and drug-stimulated ATPase activities

The beryllium-fluoride-sensitive ATPase activity of membranes, prepared from resistant ABCG2-overexpressing HEK-293 cells, was altered upon point mutations, both in the absence or presence of drug substrate (Fig. 6). While the basal ATP hydrolysis (14.6 nmol Pi/min.mg protein) was decreased (up to 30%) for the S353A mutant, L352A and S353A mutants showed at least a 3-fold decrease in the K_m values for ATP hydrolysis (Fig. 6A). More strikingly, the stimulation of basal ATPase activity in the wild-type protein by transport substrates such as nilotinib [31] was completely abolished in L352A and S353A mutants (Fig. 6B), whereas nilotinib still stimulated the ATPase activity of G354A and E356A mutants.

Alterations of the interaction with different types of drug-efflux inhibitors

The point-mutation effect on the efficiency of different types of inhibitors was studied with S353A, the most altered mutant, in comparison with wild-type ABCG2 (Fig. 7). The inhibition of mitoxantrone efflux by Ko143, an ABCG2-selective and highly-potent inhibitor [32] known to also inhibit the basal ATPase activity [33] and not to be transported, was found here to be strongly impaired in this mutant. The EC_{50} of Ko143 [34] and chromone 1 [27], which are known to inhibit ABCG2-mediated mitoxantrone efflux, was increased from 0.06 to 0.26 μ M (4.3-fold increase) and from 0.11 to 0.39 μ M (3.5-fold increase), respectively (Fig. 7A and 7B). By contrast, no significant alteration in the EC_{50} values was observed for the inhibition of activity by nilotinib, a competitive inhibitor [35] known to be transported by ABCG2 [31] (Fig. 7C).

Discussion

This paper demonstrates the functional role of a selective sequence of human ABCG2, identified as a potential extra ATP-binding motif, and its unique implication in the coupling mechanism between ATP hydrolysis and drug-efflux activity.

The ABCG2-selective C2-sequence as an additional C-motif?

Three different approaches have identified the C2-sequence LSGGE, at 352-356 positions of human ABCG2, as a possible nucleotide-binding motif. First, sequence alignment unambiguously showed complete agreement with the consensus sequence of the canonical C-motif/ABC signature found in all NBDs; second, disorder and secondary-structure predictions indicate the C2-sequence to be located between an α -helix and a loop similarly to the canonical C-motif; third, the strong

alterations induced upon point-mutations further confirmed a critical function, associated to both ATPase and drug-efflux activities.

This suggests that the C2-sequence, belonging to the linker connecting NBD and TMD, might be possibly located close to the ATP-binding site of the NBD to directly interact with bound nucleotide. The C2-sequence, at positions 352-356, is distant by about 40 residues from the beginning of TMD, which is similar to the length of the intracellular loops in crystallized bacterial Sav1866 [12] and eukaryotic P-glycoproteins [10, 11]. However, it not known if the presence of the C2-sequence might compensate the lack of a long intracellular loop, as shown in the human ABCG2 molecular model [36], or if such a multidrug homodimeric half-transporter might require additional interactions than full-transporters such as ABCB1 and ABCC1. It is not either known if the absence of such a C2-sequence in lower eukaryotes might be correlated to differences in the regulation of activity or in structural divergence of these ABCG2 homologs.

A critical function of the C2-sequence

Single-point mutations have allowed here the identification of two types of dramatic functional alterations. The first type concerned the ATPase activity, for which a decrease in both V_{\max} and K_m for ATP hydrolysis was observed; this suggested a role of the C2-sequence in either ATP binding or in ADP release, which is known to be often a rate-limiting step of ATP hydrolysis for various ATPases. In addition, the complete abolition of drug-induced stimulated ATP hydrolysis, recognized as coupling ATPase activity, was consistent with the strong catalytic impairment observed upon C-motif point-mutations in various ABC transporters, such as the second glycine in either only P-glycoprotein NBD1 [13] or both MRP1 NBD1 and NBD2 [15], the two serines in both P-glycoprotein NBD1 and NBD2 [14], and either

single glycine or glutamine in homodimeric MalK [18]. For TAP1/TAP2 heterodimer, it was demonstrated, by point-mutations within both monomers and C-motifs exchange in chimeras, that the strong alterations observed on substrate transport were correlated to changes in ATP hydrolysis [17], and not to ATP binding [16], and that the natural substitutions in degenerated TAP2 (AA *versus* SG in canonical TAP1) allowed the control of transport activity and coupled ATP hydrolysis [17]. It is not known whether residues of the ABCG2 C2-sequence might additionally establish protein-protein interactions contributing to the closure/dimerization of NBDs as shown for the C-motif within the crystal structure of HlyB [19]. The much stronger consequences induced on coupled *versus* basal ATPase indicates that both activities obey distinct mechanisms, as previously concluded from different approaches with either ABCG2 [34] or P-glycoprotein [37].

The second type of alteration concerned drug-efflux activity: i) the complete loss of cellular resistance to mitoxantrone cytotoxicity, upon 3-day culturing, appeared to contrast with the only partial decrease of mitoxantrone efflux observed in short-term flow-cytometry experiments. Different hypothetical explanations might be considered, such as time-dependent amplification under cell-culture conditions of the initially moderate alteration of drug efflux, changed IC₅₀ values of mitoxantrone for its target, or mitoxantrone-induced lowered metabolic activity of mutant cells reducing ATP concentration below threshold for basal ATPase activity (?). A marked alteration in substrate transport was also observed upon TAP1/TAP2 mutations, as mentioned above [16, 17]. Since the same C2-sequence point mutations induced a complete, primary, alteration of coupled ATP hydrolysis, the alterations observed on drug efflux might be considered as consequences, or secondary effects, rather than a direct contribution of mutated residues; ii) the strong alteration of the potent, selective, and noncompetitive Ko143 and chromone 1 inhibitors [34], known to inhibit basal ATPase

activity, suggested (despite their high hydrophobicity) a rather “cytosolic” inhibitor-binding site, in close proximity to the NBDs where ATP binds, although a distant conformational change cannot be excluded. The interaction of these inhibitors with the selective C2-sequence might, at least partly, explain their ABCG2 selectivity *versus* the other multidrug ABC transporters P-glycoprotein/ABCB1 and MRP1/ABCC1.

It may be concluded that the C2-sequence, especially L352 and S353 in human ABCG2, plays a unique role in coupling ATP hydrolysis to drug efflux, and related conformational changes of the transporter. This might constitute a new selective target to antagonize multidrug resistance in ABCG2-overexpressing cancer cells.

Acknowledgments

Drs. A. Ahmed-Belkacem and C. Gauthier are acknowledged for their help in initiating the studies and performing some experiments, respectively. This work was supported by the CNRS and University Lyon 1 (UMR 5086), and the Ligue Nationale contre le Cancer (Equipe Labellisée Ligue 2014) to A.D.P. S.M. was recipient of fellowships from the Ligue de la Loire contre le Cancer, the Association pour la Recherche sur le Cancer and the Région Rhône-Alpes (Explora'Doc mobility program with S.E.B.). R.W.R., S.S., S.V.A. and S.E.B. were supported by the Intramural Research Program of the NIH, National Cancer Institute, Center for Cancer Research. The authors also thank research funding from OTKA K 111678 and the Bolyai Fellowship of the Hungarian Academy of Sciences to T.H.

References

1. Allikmets R, Schriml LM, Hutchinson A, Romano-Spica V, Dean M (1998) A human placenta-specific ATP-binding gene (ABCP) on chromosome 4q22 that is involved in multidrug resistance. *Cancer Res* 58(23):5337-5339
2. Doyle LA, Yang W, Abruzzo LW, Krogmann T, Gao Y, Rishi AK, Ross DD (1998) A multidrug resistance transporter from human MCF-7 breast cancer cells. *Proc Natl Acad Sci USA* 95(26):15665-15670
3. Miyake K, Mickley L, Litman T, Zhan Z, Robey R, Cristensen B, Brangi M, Greenberger L, Dean M, Fojo T, Bates SE (1999) Molecular cloning of cDNAs which are highly expressed in mitoxantrone-resistant cells : demonstration of homology to ABC transport genes. *Cancer Res* 59(1):152-162
4. Juliano RL, Ling V (1976) A surface glycoprotein modulating drug permeability in Chinese hamster ovary cell mutants. *Biochim Biophys Acta* 455(1):8-13
5. Ueda K, Clark DP, Chen CJ, Roninson IB, Gottesman MM, Pastan I (1987) The human multidrug resistance (mdr1) gene. cDNA cloning and transcription initiation. *J Biol Chem* 262(2):505-508
6. Cole SP, Bhardwaj G, Gerlach JH, Mackie JE, Grant CE, Almquist KC, Stewart AJ, Kurz EU, Duncan AM, Deeley RG (1992) Overexpression of a transporter gene in a multidrug-resistant human lung cancer cell line. *Science* 258(5088):1650-1654
7. Jonker JW, Buitelaar M, Wagenaar E, van de Valk MEA, Scheffer GL, Scheper RJ, Plosch T, Kuipers F, Elferink RP, Rosing H, Beijnen JH, Schinkel AH (2002) The breast cancer resistance protein protects against a major chlorophyll-derived dietary phototoxin and protoporphyria. *Proc Natl Acad Sci USA* 99(24):15649-15654

- 1 8. Sarkadi B, Homolya L, Szakacs G, Varadi A (2006) Human multidrug resistance
2 ABCB and ABCG transporters: participation in a chemoimmunity defense
3 system. *Physiol Rev* 86(4):1179-1236
4
5
6
- 7 9. Zhou S, Morris JJ, Barnes Y, Lan L, Schuetz JD, Sorrentino BP (2002) Bcrp1
8 gene expression is required for normal numbers of side population stem cells in
9 mice, and confers relative protection to mitoxantrone in hematopoietic cells in
10 vivo. *Proc Natl Acad Sci USA* 99(19):12339-12344
11
12
13
14
15
16
- 17 10. Aller SG, Yu J, Ward A, Weng Y, Chittaboina S, Zhuo R, Harrell PM, Trinh YT,
18 Zhang Q, Urbatsch IL, Chang G (2009) Structure of P-glycoprotein reveals a
19 molecular basis for ply-specific drug binding. *Science* 323(5922):1718-1722. doi:
20 [10.1126/science.1168750](https://doi.org/10.1126/science.1168750)
21
22
23
24
25
26
- 27 11. Jin MS, Oldham ML, Chen J (2012) Crystal structure of the multidrug transporter
28 P-glycoprotein from *Caenorhabditis elegans*. *Nature* 490(7421):566-569. doi:
29 [10.1038/nature.11448](https://doi.org/10.1038/nature.11448)
30
31
32
33
- 34 12. Dawson RJ, Locher KP (2006) Structure of a bacterial multidrug ABC transporter.
35 *Nature* 443(7108):180-185
36
37
38
- 39 13. Bakos E, Klein I, Welker E, Szabo K, Muller M, Sarkadi B, Varadi A (1997)
40 Characterization of the human multidrug resistance protein containing mutations
41 in the ATP-binding cassette signature region. *Biochem J* 323(Pt 3):777-783
42
43
44
45
- 46 14. Tomblin G, Bartholomew L, Gimi K, Tyndall GA, Senior AE (2003) Synergy
47 between conserved ABC signature Ser residues in P-glycoprotein catalysis. *J*
48 *Biol Chem* 279(7):5363-5373
49
50
51
52
- 53 15. Szentpetery Z, Kern A, Liliom K, Sarkadi B, Varadi A, Bakos E (2004) The role of
54 the conserved glycines of ATP-binding cassette signature motifs of MRP1 in the
55 communication between the substrate-binding site and the catalytic centers. *J*
56 *Biol Chem* 279(40):41670-41678
57
58
59
60
61
62
63
64
65

16. Hewitt EW, Lehrer PJ (2003) The ABC-transporter signature motif is required for peptide translocation but not peptide binding by TAP. *Eur J Immunol* 33(2):422-427
17. Chen M, Abele R, Tampé R (2004) Functional non-equivalence of ATP-binding cassette signature motifs in the transporter associated with antigen processing (TAP). *J Biol Chem* 279(44):46073-46081
18. Schmees G, Stein A, Hunke S, Landmesser H, Schneider E (1999) Functional consequences of mutations in the conserved “signature sequence” of the ATP-binding cassette protein MalK. *Eur J Biochem* 266(2):420-430
19. Zaitseva J, Jenewein S, Jumpertz T, Holland IB, Schmitt L (2005) H662 is the linchpin of ATP hydrolysis in the nucleotide-binding domain of the ABC transporter HlyB. *EMBO J* 24(11):1901-1910
20. The UniProt Consortium (2015) UniProt: a hub for protein information. *Nucleic Acids Res* 43: D204-D212
21. Larkin MA, Blackshields G, Brown NP, Chenna R, McGettigan PA, McWilliam H, Valentin F, Wallace IM, Wilm A, Lopez R, Thompson JD, Gibson TJ, Higgins DG (2007) ClustalW and ClustalX version 2. *Bioinformatics* 23(21): 2947-2948
22. Rice P, Longden I, Bleasby A (2000) EMBOSS: The European Molecular Biology Open Software Suite. *Trends in Genetics* 16(6):276-277
23. Ward JJ, Sodhi JS, McGuffin LJ, Buxton BF and Jones DT (2004) Prediction and functional analysis of native disorder in proteins from the three kingdoms of life. *Journal of Molecular Biology* (337):635-645
24. Dosztányi Z, Csizmók V, Tompa P, Simon I (2005) The Pairwise Energy Content Estimated from Amino Acid Composition Discriminates between Folded and Intrinsically Unstructured Proteins. *J Mol Biol* 347:827-839

25. Cole C, Barber JD, Barton GJ (2008) The Jpred 3 secondary structure prediction server. *Nucleic Acids Research* 36:W197-W201
26. Buchan DWA, Minneci F, Nugent TCO, Bryson K, Jones DT (2013) Scalable web services for the PSIPRED Protein Analysis Workbench. *Nucleic Acids Research* 41:W340-W348
27. Valdameri G, Genoux-Bastide E, Peres E, Gauthier C, Guitton J, Terreux R, Winnischofer SM, Rocha ME, Boumendjel A, Di Pietro A (2012) Substituted chromones as highly potent nontoxic inhibitors, specific for the breast cancer resistance protein. *J Med Chem* 55(2):966-970. doi: [10.1021/jm201404w](https://doi.org/10.1021/jm201404w)
28. Morisaki K, Robey RW, Ozvegy-Laczka C, Honjo Y, Polgar O, Steadman K, Sarkadi B, Bates SE (2005) Single nucleotide polymorphisms modify the transporter activity of ABCG2. *Cancer Chemother Pharmacol* 56(2):161-172
29. Mosmann T (1983) Rapid colorimetric assay for cellular growth and survival. Application to proliferation and cytotoxicity assays. *J Immunol Methods* 65(1-2):55-63
30. Shukla S, Robey RW, Bates SE, Ambudkar SV (2006) The calcium-channel blockers, 1,4-dihydropyridines, are substrates of the multidrug resistance-linked ABC drug transporter, ABCG2. *Biochemistry* 45(29):8940-8951
31. Shukla S, Skoumbourdis AP, Walsh MJ, Hartz AM, Fung KL, Wu CP, Gottesman MM, Bauer B, Thomas CJ, Ambudkar SV (2011) Synthesis and characterization of a BODIPY conjugate of the BCR-ABL kinase inhibitor Tasigna (nilotinib): evidence for transport of Tasigna and its fluorescent derivative by ABC drug transporters. *Mol Pharmaceut*. 8(4):1292-1302. doi: [10.1021/mp2001022](https://doi.org/10.1021/mp2001022)
32. Allen JD, van Loevezijn A, Lakhai JM, van der Valk M, van Tellingen O, Reid G, Schellens JH, Koomen GJ, Schinkel AH (2002) Potent and specific inhibition of

- the breast cancer resistance protein multidrug transporter in vitro and in mouse intestine by a novel analogue of fumitremorgin C. *Mol Cancer Ther* 1(6):417-425
33. Ozvegy-Laczka C, Hegedus T, Varady G, Ujhelly O, Schuetz JD, Varadi A, Keri G, Orfi L, Nemet K, Sarkadi B (2004) High-affinity interaction of tyrosine kinase inhibitors with the ABCG2 multidrug transporter. *Mol Pharmacol* 65(6):1485-1495
34. Winter E, Lecerf-Schmidt F, Jabor Gozzi G, Peres B, Lightbody M, Gauthier C, Ozvegy-Laczka C, Sarkadi B, Creczynski-Pasa TB, Boumendjel A, Di Pietro A (2013) Structure-activity relationships of chromone derivatives toward mechanism of interaction with, and inhibition of, breast cancer resistance protein ABCG2. *J Med Chem* 56(24):9849-9860. doi: [10.1021/jm401649j](https://doi.org/10.1021/jm401649j)
35. Tiwari AK, Sodani K, Wang SR, Kuang YH, Ashby CR Jr, Chen X, Chan ZS (2009) Nilotinib (AMN107, Tasigna) reverses multidrug resistance by inhibiting the activity of the ABCB1/Pgp and ABCG2/BCRP/MXR transporters. *Biochem Pharmacol* 78(2):153-161. doi: [10.1016/j.bcp.2009.04.002](https://doi.org/10.1016/j.bcp.2009.04.002)
36. Hazai E, Bikadi Z (2008) Homology modeling of breast cancer resistance protein (ABCG2). *J Struct Biol* 162(1):63-74. doi: [10.1016/j.jsb.2007.12.001](https://doi.org/10.1016/j.jsb.2007.12.001)
37. Al-Shawi MK, Polar MK, Omote H, Figler RA (2003) Transition state analysis of the coupling of drug transport to ATP hydrolysis by P-glycoprotein. *J Biol Chem* 278(52):52629-52640

Figure captions

Fig. 1. Sequence alignment of human ABCG sub-family members, emphasizing the regions containing the canonical signature/C-motif (marked with a blue line) (**A**) or a non-canonical C2-sequence that is only present in ABCG2 (marked with red line) (**B**). Alignment of the linker region containing the non-canonical C2-sequence of human ABCG2 with homologous regions of ABCG2 homologs from various species (**C**).

Fig. 2. Predictions of disorder within the linker region of human ABCG2 containing the LSGGE C2-sequence at positions 352-356. The arrows show the C2-sequence position.

Fig. 3. Detection and quantification of the C2-sequence point mutants within the plasma membrane of transfected cells by flow cytometry with the 5D3 surface antibody. Stably-transfected HEK293 cells were incubated with phycoerythrin-labeled 5D3 antibody (blue line) or a negative control antibody (red line) (**A**). Similarly to wild-type ABCG2, the C2-sequence mutants and the R482G gain-of-function mutant were detected on the cell surface, and quantified by 5D3 fluorescence; the bars represent the mean of median fluorescence (**B**). HEK293 cells with stable expression of either pcDNA3.1 empty vector, wild-type ABCG2 or the C2-sequence L352A mutant were fixed and immunostained with the ABCG2-specific BXP-21 antibody, and nuclei were counterstained with 4',6-diamidino-2-phenylindole (DAPI) (**C**).

Fig. 4. Mutation-induced alterations of ABCG2-mediated drug-efflux activity. HEK293 cells expressing wild-type ABCG2, the different C2-sequence mutants or the R₄₈₂G gain-of-function mutant were incubated with 20 μ M mitoxantrone with (blue line) or without (red line) 10 μ M fumitremorgin C (FTC) as a specific inhibitor, to generate the

histograms (**A**). The efflux was quantified by difference between the two histograms either without further corrections (**B**) or by taking into account the exact plasma membrane ABCG2 content determined in Fig. 3B (**C**).

Fig. 5. Mutation-induced sensitization to mitoxantrone toxicity of the growth of multidrug-resistant cells. The different sensitivities to mitoxantrone of transfected HEK293 cells with stable expression of wild-type ABCG2 (in green) or the control pcDNA3.1 empty vector (in magenta) were compared to that of ABCG2 mutants (in black) with the following point mutations: L352A (**A**), S353A (**B**), G354A (**C**) or E356A (**D**). The cells were cultured on monolayer at day 0, and increasing concentrations of mitoxantrone were added to cells at day 1 until day 5; they were stained with MTT, and the absorbance read at 570 nm. Data points represent mean values \pm SD (n = 3).

Fig. 6. Differential mutation-induced alterations of basal (**A**) and substrate-stimulated (**B**) ATPase activity of ABCG2. (**A**) Crude membranes from transfected HEK293 cells expressing wild-type ABCG2, or the L352A, S353A or E356A mutant were incubated in the presence or absence of beryllium-fluoride (0.2 mM beryllium sulfate and 2.5 mM sodium fluoride) in ATPase assay buffer with increasing ATP concentrations in the absence of substrate drug. (**B**) The drug-stimulated activity was measured at 5 mM ATP upon addition of 0.25 μ M nilotinib (grey bars) in comparison to the basal activity without substrate addition (black bars). The results are expressed as mean values \pm standard deviations from three independent experiments.

Fig. 7. Mutation-induced alterations of ABCG2 interaction with different types of inhibitors. The efflux of mitoxantrone by HEK293 cells expressing either wild-type

ABCG2 (circles) or the S353A mutant (triangles) was measured by flow cytometry as in Fig. 4. Its inhibition by increasing concentrations of Ko143 (**A**), chromone 1 (**B**) or nilotinib (**C**) was plotted as indicated.

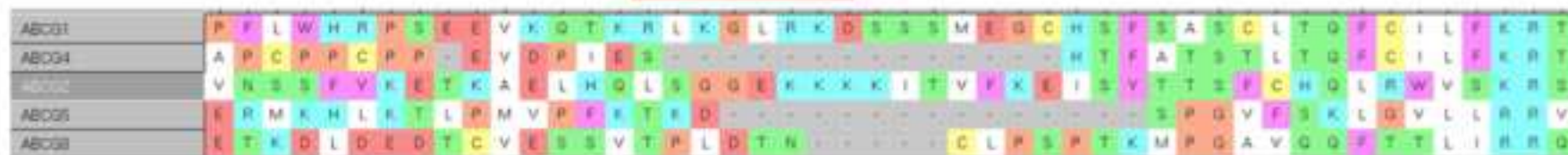
Canonical signature

A



Non-canonical signature

B



C

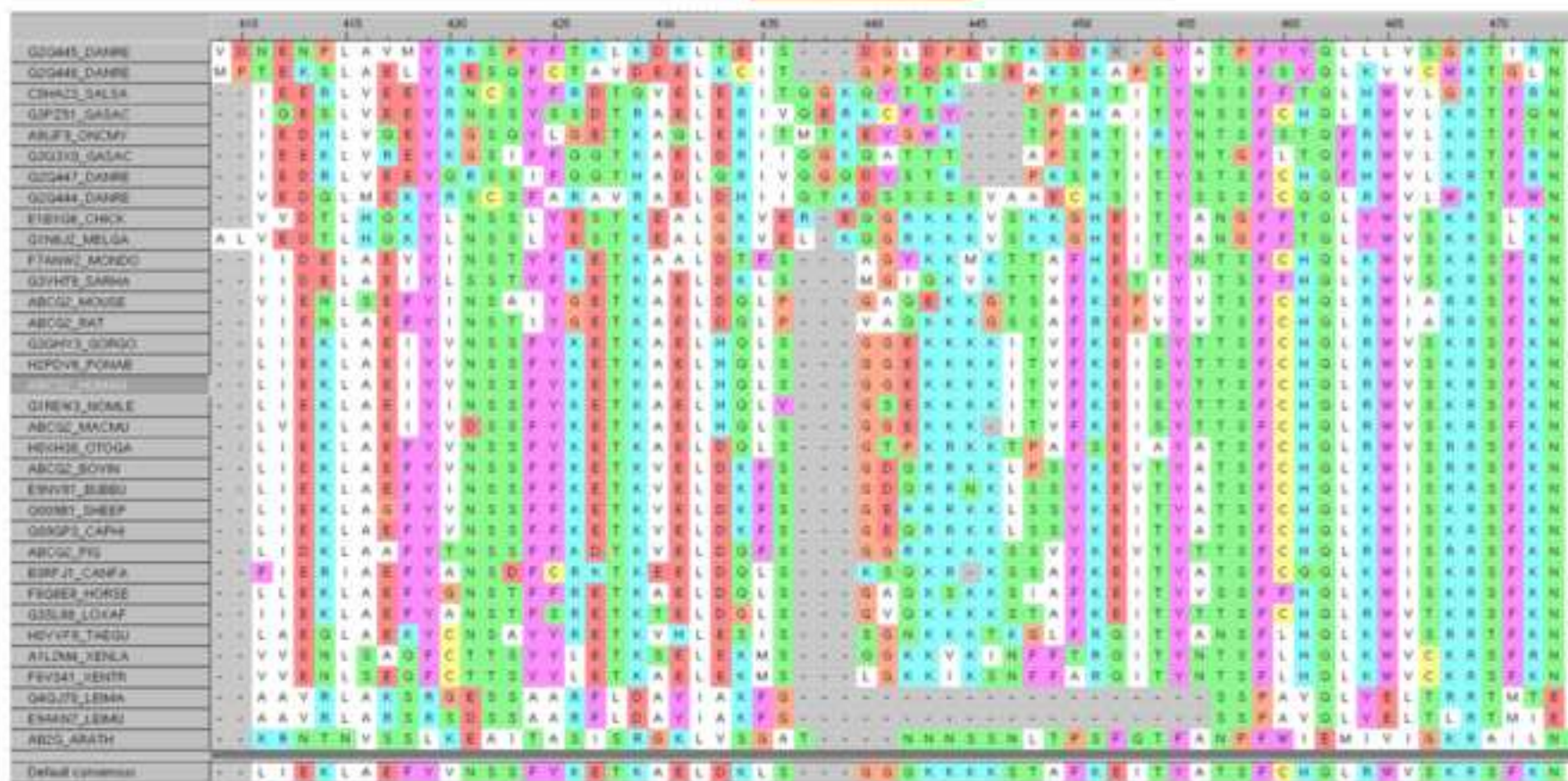


Figure 2

[Click here to download Figure Figure_2.tif](#)

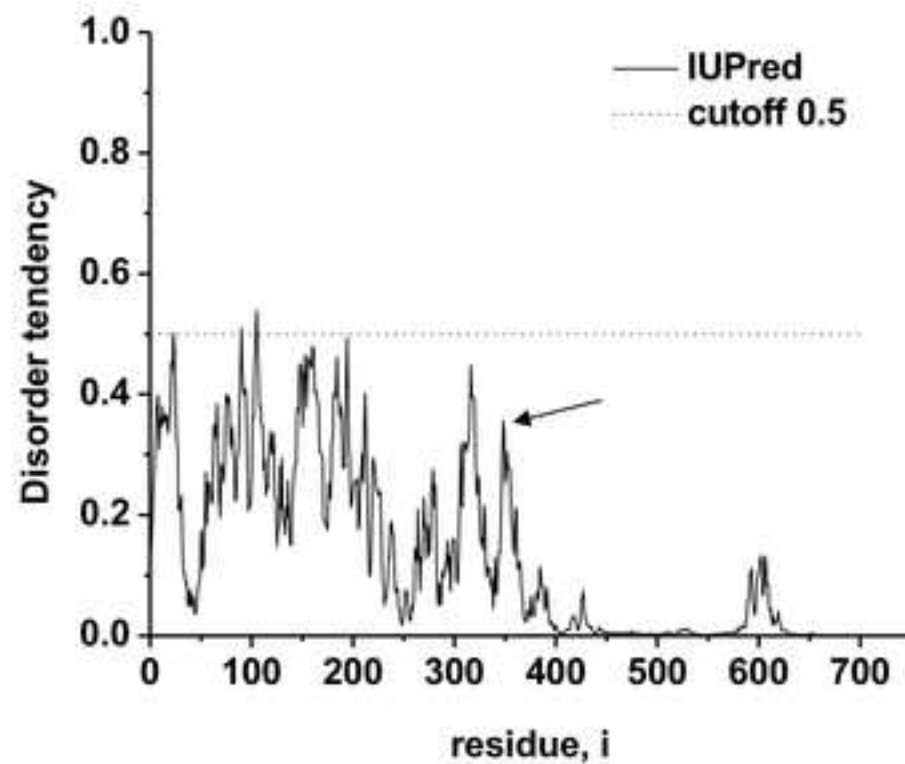
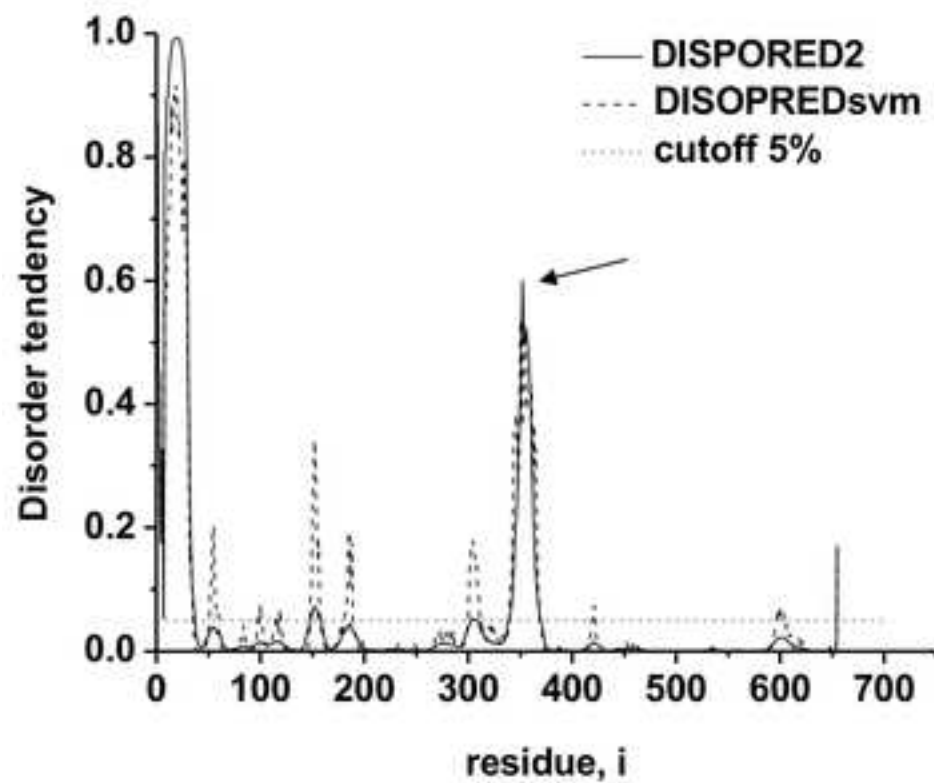


Figure 3

[Click here to download Figure_3.tif](#)

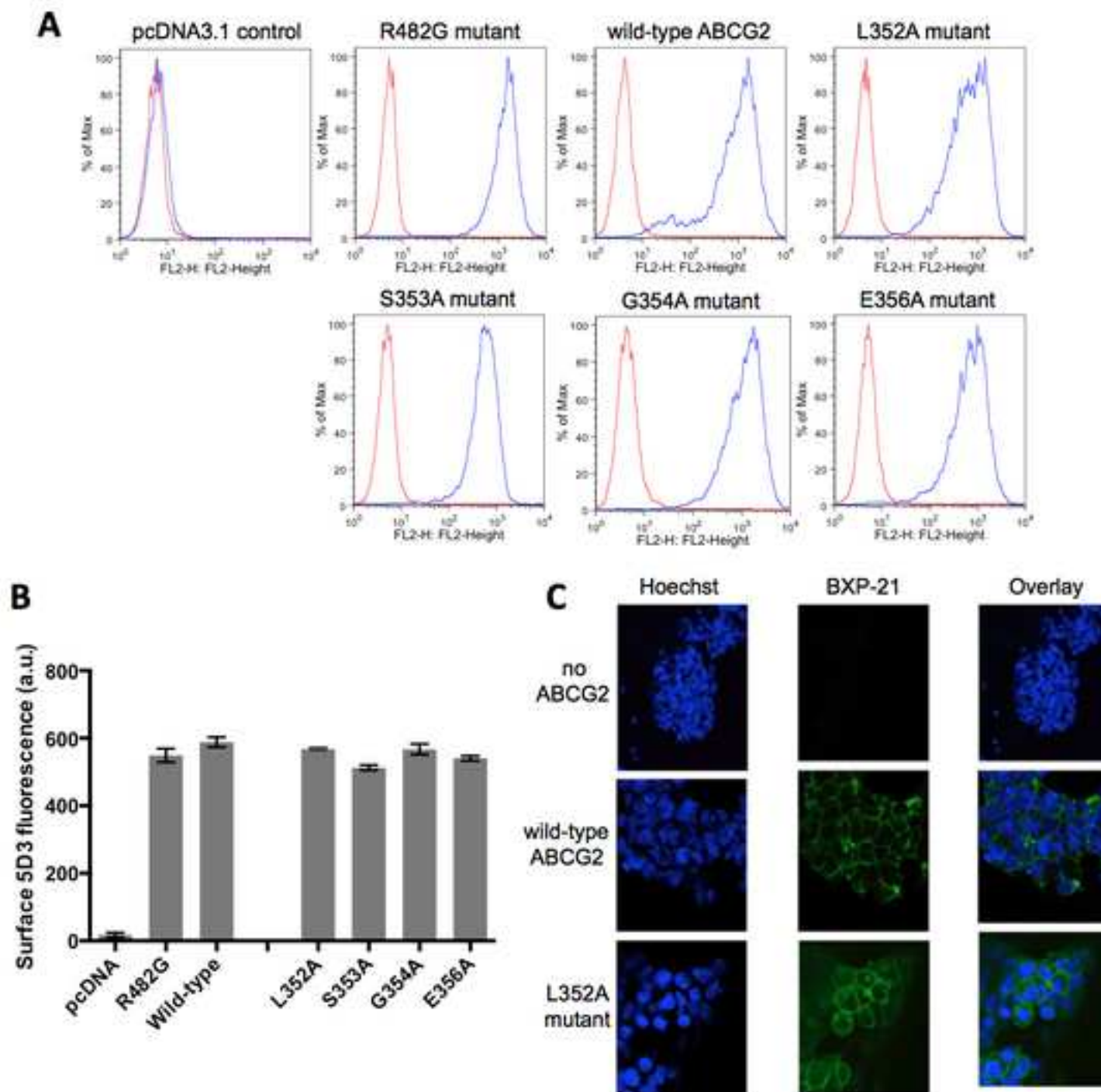


Figure 4

[Click here to download Figure_4.tif](#)

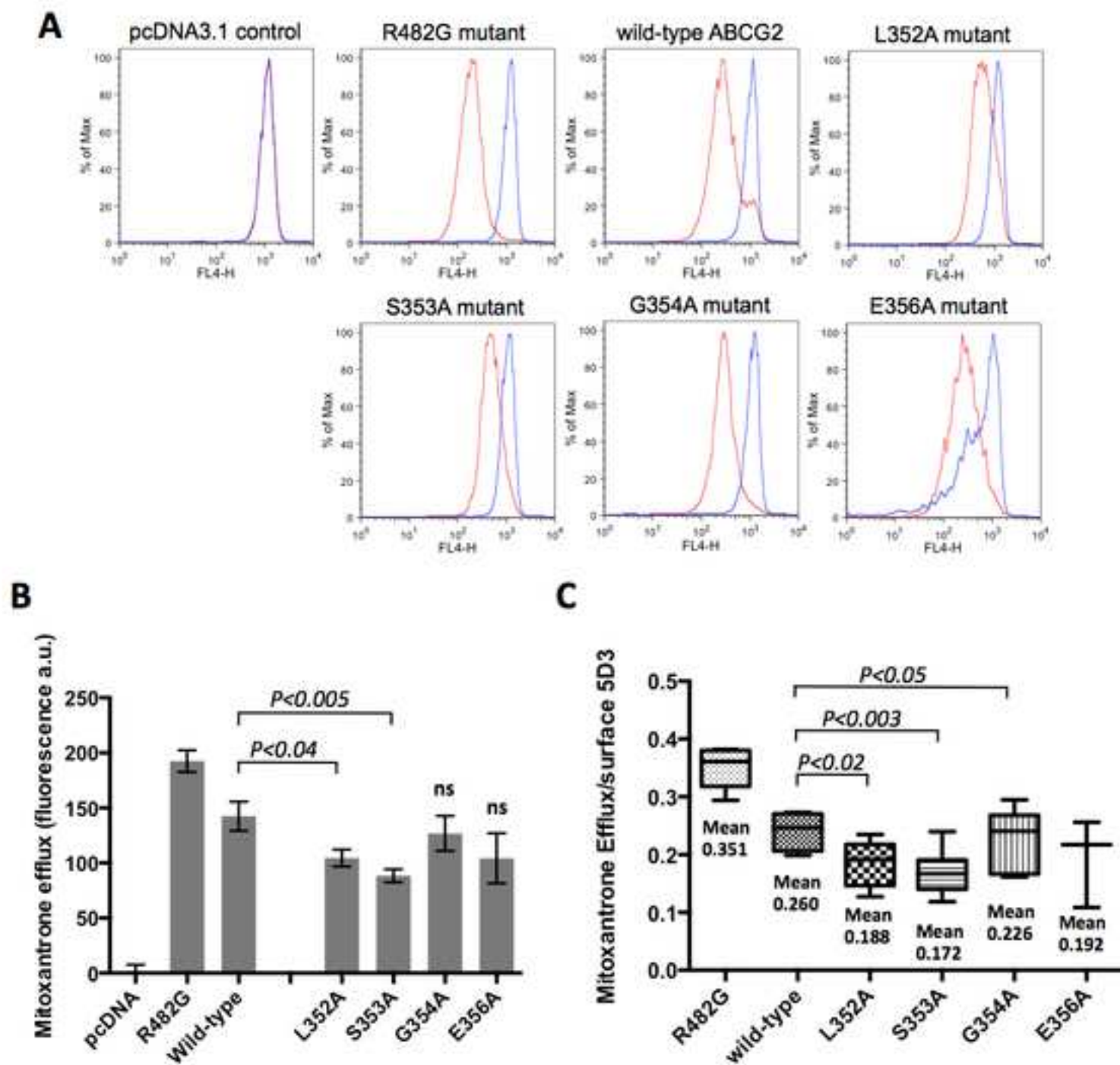
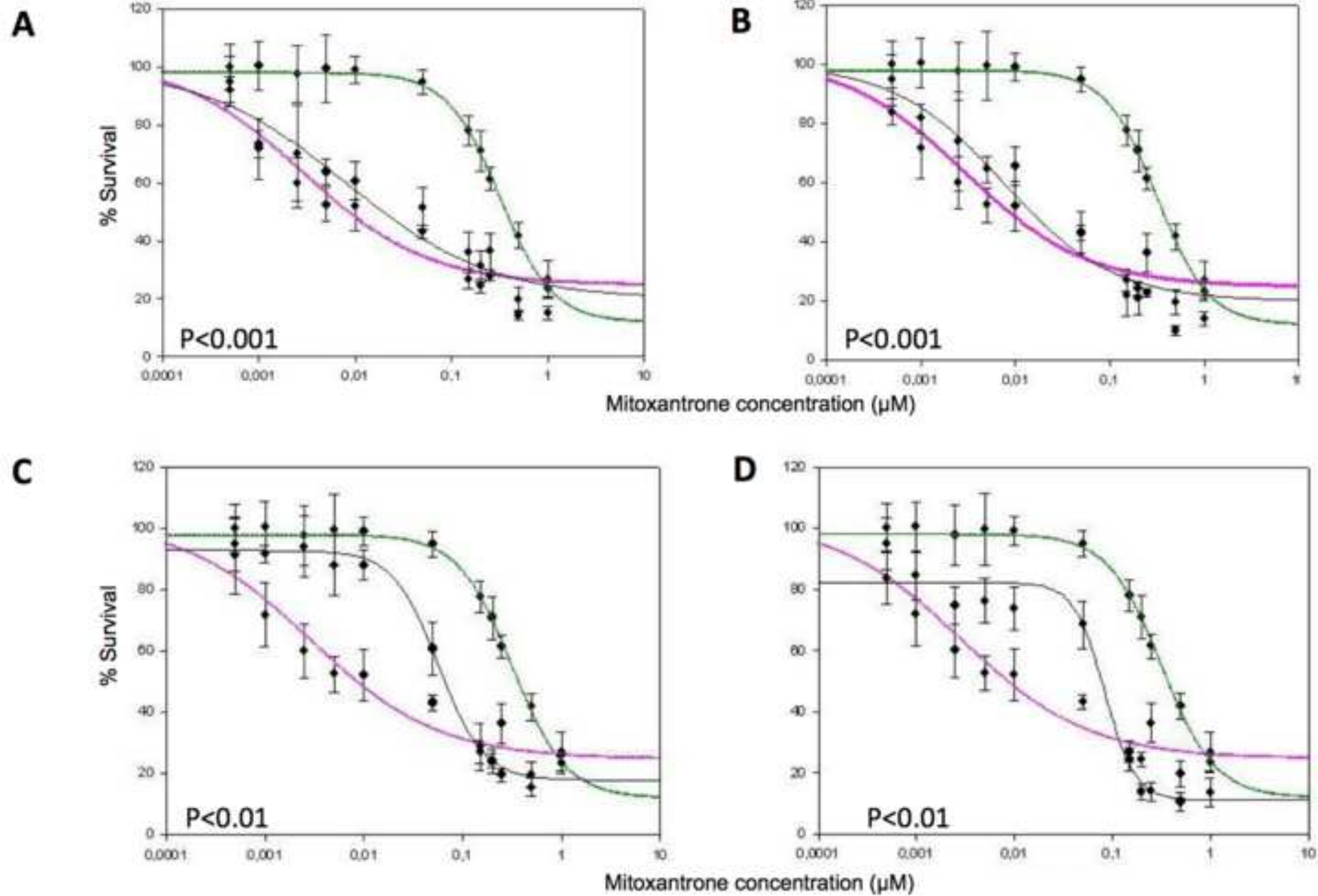


Figure 5

[Click here to download Figure_5.tif](#)



A

	Wild-type ABCG2	L352A mutant	S353A mutant	E356A mutant
V_{max} (nmol Pi/ mg protein.min)	14.6	11.3	10.2	11.1
K_m ATP (mM)	0.45	0.15	0.06	0.46

B

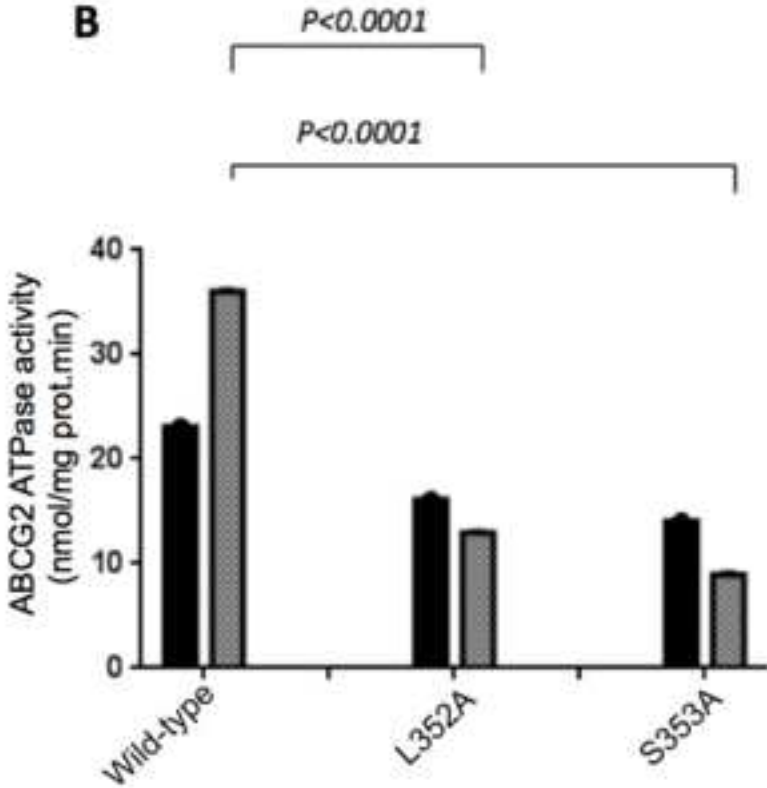
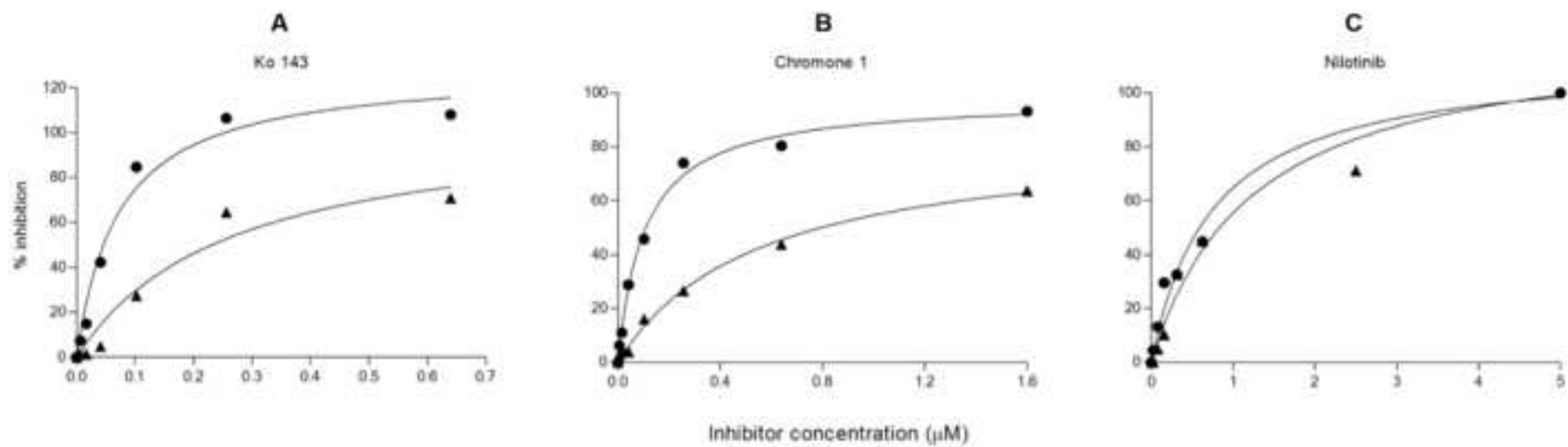


Figure 7





Click here to access/download
Supplementary Material
Answers_to_Reviewers.doc